Available online at www.sciencedirect.com
ScienceDirect
Thermochimica Acta 465 (2007) 25–29
thermochimica acta
www.elsevier.com/locate/tca

Heat capacities of $RCoO_3$(s) (R = La, Nd, Sm Eu, Gd, Tb, Dy and Ho) by differential scanning calorimetry

Abhay Patil, S.C. Parida *, Smruti Dash, V. Venugopal

Product Development Section, Radiochemistry and Isotope Group, Bhabha Atomic Research Centre, Mumbai 400085, India

Received 20 April 2007; received in revised form 31 August 2007; accepted 6 September 2007
Available online 14 September 2007

Abstract

Ternary oxides, $RCoO_3$(s) (R = La, Nd, Sm Eu, Gd, Tb, Dy and Ho), have been prepared by citrate–nitrate gel combustion route and characterized by X-ray diffraction analysis. Heat capacities of these compounds have been measured in the temperature range from 130 to 850 K using a heat flux type differential scanning calorimeter. Heat capacity versus temperature plots for these compounds indicated broad humps in the temperature range from 450 to 780 K suggesting electronic transitions in these compounds accompanied by large entropy increments. The transition temperatures showed increasing trend with decrease in ionic radii of the lanthanide ion.

Keywords: Rare-earth cobalt oxides; Perovskites; Heat capacity; Electronic transition; Differential scanning calorimetry

1. Introduction

Ternary oxides of rare-earth and transition metals are important because of their electrical, magnetic and catalytic properties. Some of the RMO_3 (R = lanthanide elements, M = transition metal) compounds are used as electrode materials for magnetohydrodynamics (MHD) generators [1], fuel cells [2] and as catalysts for oxidation of CO [3]. The cobalt containing perovskites, $RCoO_3$, are used as precursors of the catalyst for the partial oxidation of methane to synthesis gas [4]. These perovskites offer high activity and selectivity in the catalytic process. Heterojunctions of RMO_3/SnO_2 are also being explored as gas sensors [5,6]. Tsuyoshi et al. [7] have discussed the gas sensing mechanism of rare-earth cobaltites from conductivity data. Moon et al. [8] have discussed the thermoelectric behavior of $RCoO_3$-type perovskite oxides. $NdCoO_3$(s) and $GdCoO_3$(s) show high Seebeck coefficients in the vicinity of room temperature and hence expected to have unique thermoelectric properties [8]. The authors [8] have evaluated the electrical conductivity, Seebeck coefficients and thermal conductivities of partially Ca-doped $RCoO_3$(s) oxides as a function of temperature.

The successful use of these oxide materials in technical processes is in many respects limited by the knowledge of their thermodynamic stability. The phase transition temperatures and the nature of phase transitions are also important in many respects. Raccah and Goodenough [9] have studied the first-order localized-electron to collective-electron transition in $LaCoO_3$(s) using structural, calorimetric, magnetic, electrical conductivity and thermal conductivity data. They have reported a first-order transition at 1210 K, a higher order transition in the temperature interval $398 < T\,(\mathrm{K}) < 648$, another higher order transition at about 923 K. Bhide et al. [10,11] have carried out Mössbauer studies of the high-spin–low-spin equilibria and the localized-collective electron transition in $LaCoO_3$(s) in the 4.2–1200 K temperature range and reported that cobalt ion exist predominantly in the low-spin Co^{III} state at low temperatures which transforms partially to high-spin Co^{3+} ions up to 200 K. At high temperatures, the population of Co^{3+} decreases and completely disappears at the localized-collective-electron transition temperature at 1210 K [10,11]. Rajoria et al. [12] have studied the spin state equilibria and localized versus collective d-electron behavior in $NdCoO_3$(s) and $GdCoO_3$(s) by magnetic susceptibility and Mössbauer measurements and concluded that the first-order transition occurs around 1000 K. Bose et al. [13] have studied the spin-state equilibria in the $RCoO_3$(s) system from ^{59}Co NMR in the temperature range 110–550 K and confirmed the coexistence of the high-spin–low-spin state.

* Corresponding author. Tel.: +91 22 2559 0648; fax: +91 22 2550 5151.
E-mail address: sureshp@barc.gov.in (S.C. Parida).

0040-6031/$ – see front matter © 2007 Elsevier B.V. All rights reserved.
doi:10.1016/j.tca.2007.09.001

Bortolome et al. [14] have measured the low-temperature specific heat of $NdCoO_3$(s) in the 200 mK to 5 K temperature range and revealed the magnetic ordering on Nd ions. Stølen et al. [15,16] have discussed the energetics of spin transition in $LaCoO_3$(s) from heat capacity data measured in the temperature range from 13 to 1000 K by adiabatic calorimetry. The authors [15,16] have reported a spin transition between 20 and 100 K and another transition in the vicinity of 530 K. Abbate et al. [17] have studied the spin-state transition using high-resolution soft X-ray-absorption spectroscopy and X-ray photoelectron spectroscopy. The authors [17] have confirmed that the low-spin to high-spin transition in $LaCoO_3$(s) occurs in the region $400 < T\ (K) < 650$. Ravindran et al. [18] have studied the electronic structure of the Sr-substituted $LaCoO_3$(s) by a series of generalized-gradient-corrected, full-potential, spin-density-functional band structure calculations. The authors [18] have accounted for the spin-state transition from a diamagnetic state to a paramagnetic state at 100 K and from semiconductor to metal transition above ∼500 K. Nekrasov et al. [19] have studied the influence of rare-earth ion radii on the low-spin to intermediate-spin state transition in $LaCoO_3$(s) and $HoCoO_3$(s) by first-principle calculations of electronic structure and magnetic states. They have observed that the low-spin to intermediate spin state transition temperature increases with increase in rare-earth ionic radii. A survey of all the above-mentioned literature suggests that a systematic study on $RCoO_3$(s) is required for thorough understanding for the nature of spin state transition. In our opinion, heat capacity measurements on $RCoO_3$(s) from near zero to high temperature will clearly reveal the energetics of spin state transition, give accurate transition temperatures and describe the order of transition. However, a complete set of heat capacity data for all the $RCoO_3$ is not available in the literature. This study aims at measurement of heat capacities of $RCoO_3$(s) (R = La, Nd, Sm Eu, Gd, Tb, Dy and Ho) in the temperature range from 130 to 850 K and determination of their transition temperatures from heat capacity versus temperature curves.

2. Experimental

2.1. Material preparation

Ternary oxides, $RCoO_3$(s) (R = La, Nd, Sm Eu, Gd, Tb, Dy and Ho), have been prepared by citrate–nitrate gel combustion route. Preheated R_2O_3(s) (LEICO Industries Inc., USA, 0.999 mass fraction) and Co_3O_4(s) (0.999 mass fraction) with stoichiometric ratios were dissolved in 4–5 M HNO_3. Excess amount of citric acid (E. Merck, India, 0.999 mass fractions) was added to the solution. Then pH of the solution was adjusted to 6–7 by adding liquor ammonia. This solution was heated at 450 K, a viscous gel was formed which was further dried, crushed, pelletised using a steel die at a pressure of 100 MPa and heated at 1425 K in a platinum crucible for 120 h with two intermediate grindings. The products were identified by X-ray diffraction analysis using DIANO powder diffractometer with Cu Kα radiation (λ = 1.5406 Å) with Ni-filter and graphite monochromator. The diffraction patterns show that the products obtained are $LaCoO_3$(s), $NdCoO_3$(s), $SmCoO_3$(s), $EuCoO_3$(s), $GdCoO_3$(s), $TbCoO_3$(s), $DyCoO_3$(s) and $HoCoO_3$(s) (see supplementary information for the obtained X-ray diffraction patterns as shown in Fig. 1 and the relative intensities of six strongest peaks with their corresponding values of interplanar spacing (*d*) as listed in Table 1). No detectable impurity phases were observed in the X-ray diffraction pattern. The prepared samples were stored in a desiccator for heat capacity measurements.

Chemical analysis of all the samples was carried out in order to confirm the purity of the samples. A known amount of $RCoO_3$(s) sample was dissolved in concentrated HCl under hot condition. This solution was heated on a hot plate at ∼100 °C to near dryness, followed by addition of 4 M HNO_3 and heating to near dryness. This process was repeated for three to four times to ensure complete removal of chloride. The solution was made up to a known volume by 1 M HNO_3 and analysed by total reflection X-ray fluorescence (TXRF) spectroscopic method using rare-earth and cobalt standard solutions. The rare-earth to cobalt metal ratio obtained from TXRF analysis was found to be the same as the formula ratio indicating that the compounds are stoichiometric with respect to metals. The TXRF analysis also revealed that Al- and Si-bearing impurities are absent.

2.2. Measurement of heat capacity using differential scanning calorimetry

The heat flux DSC (Model: DSC 131) supplied by M/s. SETARAM instrumentations, France, was used to measure the heat capacities of all the samples. The transducer of DSC 131 has been designed using the technology of the plate-shaped DSC rods made of chromel–constantan. It is arranged in a small furnace with a metal resistor of low-thermal inertia so as to produce high heating and cooling rates, thereby providing for high-speed experiments. The transducer also possesses very good sensitivity over the whole temperature range (100–950 K). The temperature calibration of the calorimeter was carried out in the present study by the phase transition temperature of National Institute of Standards and Technology (NIST) reference materials (mercury: T_{fus} = 234.316 K; gallium: T_{fus} = 302.914 K; indium: T_{fus} = 429.748 K; tin: T_{fus} = 505.078 K; lead: T_{fus} = 600.600 K) and AR grade samples (*n*-pentane: T_{fus} = 140.490K; cyclohexane: T_{fus} = 190.0 K; 280.1 K; deionised water: T_{fus} = 273.160 K; potassium nitrate: T_{fus} = 400.850 K; silver sulfate: T_{fus} = 703.150 K; potassium sulfate: T_{fus} = 856.150 K). Heat calibration of the calorimeter was carried out by using the enthalpies of transition of the above-mentioned materials. For the determination of heat capacity, NIST synthetic sapphire (SRM 720) in the powder form was used as the reference material. Heat capacity of all the oxides were determined by the classical three-step method in the continuous heating mode in two different temperature ranges: (i) $130 \leq T\ (K) \leq 320$ and (ii) $300 \leq T\ (K) \leq 860$. Heat flow as a function of temperature was measured in the first temperature range at a heating rate of 5 K min^{-1} with high purity helium as a carrier gas with a flow rate of 2 $dm^3\ h^{-1}$. For the second temperature range, high purity argon was used as a carrier gas with the same flow rate as that of helium and same heating rate. Two flat bottom aluminum crucibles of identical masses of capacity

10^{-4} dm^3 with covering lids were used as containers for sample and reference materials. About 300–350 mg of the sample was used for the heat capacity measurements.

In DSC 131, heat capacity of the sample under investigation can be calculated by a simple comparison of the heat flow rates in three runs as illustrated in the literature [20]. The expression used for the calculation of heat capacity of the sample is given as

$$C_p(T)_{\text{sample}} = \left(\frac{\text{HF}_{\text{sample}} - \text{HF}_{\text{blank}}}{\text{HF}_{\text{ref}} - \text{HF}_{\text{blank}}}\right)\left(\frac{M_{\text{ref}}}{M_{\text{sample}}}\right) C_p(T)_{\text{ref}} \quad (1)$$

where HF_{blank}, HF_{ref} and $\text{HF}_{\text{sample}}$ represent heat flow during first, second and third runs, respectively, $C_p(T)_{\text{sample}}$ and $C_p(T)_{\text{ref}}$ the heat capacities of sample and reference material, whereas M_{sample} and M_{ref} represent the masses of sample and reference, respectively. In order to check the accuracy of the measurements the heat capacities of Fe_2O_3 (mass fraction 0.998) and NiO (mass fraction 0.999) were measured in the temperature range from 120 to 850 K and values were found to be within ±1.5% of the literature values [21].

3. Results and discussion

The heat capacity data for $RCoO_3$(s) (R = La, Nd, Sm Eu, Gd, Tb, Dy and Ho) obtained in the present study at selected temperatures are given in the supplementary data files. The variation of heat capacity as a function of temperature is shown in Fig. 1. It is evident from Fig. 1 that for all the compounds there is a broad hump in the heat capacity versus temperature plot. These broad humps in the heat capacity versus temperature plots suggest that these compounds undergo electronic transitions in a broad range of temperature. The excess heat capacity ($\Delta_{\text{exc}}C_{p,\text{m}}$) accompanied by transition can be estimated by subtracting the lattice contribution to the total isobaric heat capacity. The lattice heat capacities of $RCoO_3$(s) can be best approximated by the sum of the lattice heat capacities of constituent oxides (R_2O_3 and Co_2O_3) in their stoichiometric molar ratios as proposed by Stølen et al. [15,16]. However, Co_2O_3(s) is a high-pressure phase and its lattice heat capacity is not available in the literature. Hence, the lattice heat capacity of Fe_2O_3(s) [22] has been taken as an alternative to Co_2O_3(s). The lattice heat capacities of R_2O_3(s) have been taken from the literature [23–25]. Further, we have neglected the dilational contribution of R_2O_3(s) and Co_2O_3(s) in this calculation. Hence, the excess heat capacity calculated by this method is an approximation which may introduce an error of 3–4%. The variation of excess heat capacity ($\Delta_{\text{exc}}C_{p,\text{m}}$) as a function of temperature for $LaCoO_3$(s) is shown in Fig. 2. The excess entropy ($\Delta_{\text{exc}}S_{\text{m}}$) due to electronic transition can be calculated by integrating the area under the curve of ($\Delta_{\text{exc}}C_{p,\text{m}}/T$) versus T. For all the other $RCoO_3$(s) similar procedure is followed. The transition temperature is obtained by observing the maximum value of excess heat capacity. The excess entropies and the transition temperatures for $RCoO_3$(s) estimated by this method are given in the supplementary data file (Table 3). The maximum values of excess heat capacity are observed at 554, 610, 619, 673, 675, 735 and 741 K for $LaCoO_3$(s), $NdCoO_3$(s), $SmCoO_3$(s), $EuCoO_3$(s), $GdCoO_3$(s), $TbCoO_3$(s) and $DyCoO_3$(s), respectively. Though a broad hump was observed for $HoCoO_3$(s), its transition temperature could not be ascertained because of incomplete tail in the heat capac-

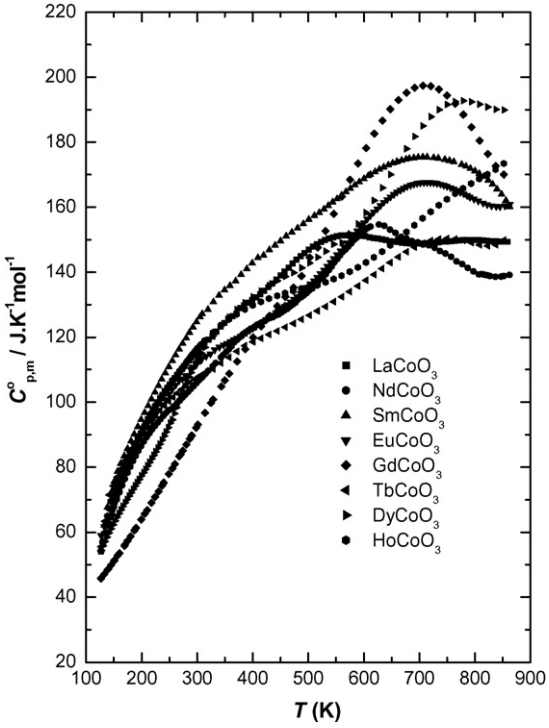

Fig. 1. Variation of heat capacities of $RCoO_3$(s) as a function of temperature.

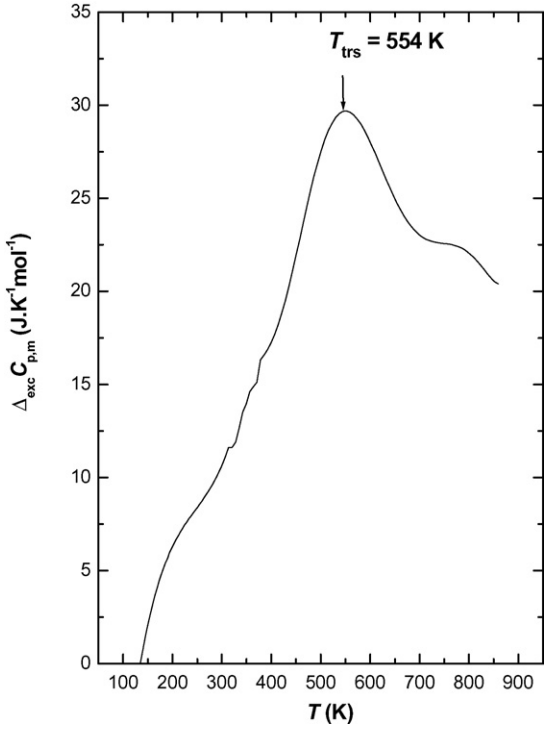

Fig. 2. Variation of excess heat capacity ($\Delta_{\text{exc}}C_{p,\text{m}}$) as a function of temperature for $LaCoO_3$(s).

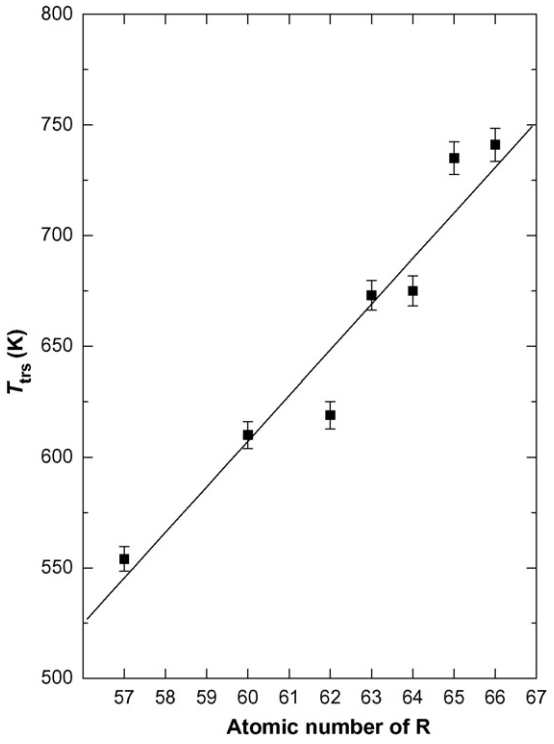

Fig. 3. Variation of transition temperature (T_{trs}) as a function of atomic number of R in $RCoO_3$(s).

ity plot obtained in the experimental temperature range. The plot of transition temperatures (T_{trs}) for the above compounds as a function of atomic number of *R* is shown in Fig. 3. It can be seen from the figure that, to a good approximation, the transition temperature increases linearly with increase in atomic number of *R*. The increase in transition temperature across the series is due to the fact that at room temperature all the cobalt ions are in the low-spin state and with increase in temperature, the excited state becomes more and more populated. However, across the series with smaller rare-earth ions, the stability of low spin state of Co-ion increases due to increase in the crystal-field energy splitting value and hence the transition temperature increases.

Stølen et al. [15,16] have prepared $LaCoO_3$(s) and measured the heat capacity from 13 to 1000 K using adiabatic calorimetric technique. The heat capacity data obtained in this study are in good agreement (within ±2%) with those of Stølen et al. [16] in the temperature range from 300 to 850 K. However, the transition temperature of $LaCoO_3$(s) obtained in this study (554 K) is higher than the value observed (530 K) by Stølen et al. [15,16]. The difference in the heat capacity maxima may be due to the fact that the measurement by Stølen et al. [15,16] is by adiabatic calorimetry which involves equilibrium measurement at discrete temperatures where as the present study involves measurement of heat capacity by DSC in a continuous heating mode. Other conditions like sample preparation, annealing temperature and impurity content may be the reason for the discrepancy in the transition temperature.

The origin of broad hump in the heat capacity plot for $LaCoO_3$(s) is due to electronic transition as described by Stølen et al. [15,16]. $LaCoO_3$(s) is a semiconductor and nonmagnetic at absolute zero temperature. As the temperature is increased, two different broad transitions have been observed by Stølen et al. [15]; one in the temperature range of $20 < T\,(K) < 100$ and the other in the temperature range of $450 < T\,(K) < 600$. The low-temperature transition is established as a spin transition, where as the higher temperature transition is a semiconductor to metal transition. As inferred by Abbate et al. [17], the low-spin (LS) state of Co^{3+} is stable below 400 K and the low-spin to high-spin (HS) transition occurs in the region $400 < T\,(K) < 650$. In the present study, the saturation of spin excitations is observed at 650 K for $LaCoO_3$(s). The excess entropy calculated from 130 to 850 K is due to the sum of various transitions taking place in $RCoO_3$(s) from low spin (LS) state to high-spin (HS) state via a stabilized intermediate spin (IS) state as explained by Stolen et al. [15], Abbate et al. [17], Ravindran et al. [18] and Nekrasov et al. [19].

The heat capacity data for other compounds are not reported in the literature for comparison. The broad heat capacity hump observed for $RCoO_3$ (R = Nd, Sm Eu, Gd, Tb, Dy and Ho) could be due to dominant magnetic interactions and interactions between magnetic and electronic transitions. However, for $LaCoO_3$(s) it is due to electronic transition. Thus, substantial entropy effect will be expected for $RCoO_3$(s) (R = Nd, Sm Eu, Gd, Tb, Dy and Ho).

A complete set of heat capacity data in the entire temperature range from near absolute zero to ∼1000 K or above will be helpful in describing fully the nature of transitions in $RCoO_3$(s) (R = La, Nd, Sm Eu, Gd, Tb, Dy and Ho) compounds.

Acknowledgements

The authors are pleased to acknowledge Dr. K. Krishnan, Fuel Chemistry Division, for X-ray diffraction analysis and Shri B.K. Sen, Head, Product Development Section for his interest in the work.

Appendix A. Supplementary data

Supplementary data associated with this article can be found, in the online version, at doi:10.1016/j.tca.2007.09.001.

References

[1] D.B. Meadowcraft, P.G. Meier, A.C. Warren, Energy Convers. 12 (1972) 145.
[2] H.S. Spacil, C.S. Tedmon Jr., J. Electrochem. Soc. 116 (1969) 1618.
[3] W.F. Libby, Science 171 (1971) 499.
[4] R. Lago, G. Bini, M.A. Pena, J.L.G. Fierro, J. Catal. 167 (1997) 198.
[5] M. Mitsuoka, A. Otofuji, T. Arakawa, Sens. Actuators B 9 (1992) 205.
[6] R. Mochinaga, T. Yamasaki, T. Arakawa, Sens. Actuators B 9 (1998) 96.
[7] A. Tsuyoshi, K. Hiroshi, S. Jiro, J. Mater. Sci. 20 (1985) 1207.
[8] J.-W. Moon, Y. Masuda, W.-S. Seo, K. Koumoto, Mater. Sci. Eng. B 85 (2001) 70.
[9] P.M. Raccah, J.B. Goodenough, Phys. Rev. 155 (1967) 932.
[10] V.G. Bhide, D.S. Rajora, G. Rama Rao, C.N.R. Rao, Phys. Rev. B 6 (1972) 1021.
[11] V.G. Bhide, D.S. Rajora, Y.S. Reddy, G. Rama Rao, G.V. Subha Rao, C.N.R. Rao, Phys. Rev. Let. 28 (1972) 1133.

[12] D.S. Rajoria, V.G. Bhide, G. Rama Rao, C.N.R. Rao, J. Chem. Soc., Faraday Trans. II 70 (1974) 512.
[13] M. Bose, A. Ghoshray, A. Basu, Phys. Rev. B 26 (1982) 4871.
[14] F. Bartolome, M.D. Kuzmin, J. Bartolome, J. Blasco, J. Garcia, F. Sapina, Solid State Commun. 91 (1994) 177.
[15] S. Stølen, F. Gronvold, H. Brinks, Phys. Rev. B 35 (1997) 14103.
[16] S. Stølen, F. Gronvold, H. Brinks, T. Atake, H. Mori, J. Chem. Thermodyn. 30 (1998) 365.
[17] M. Abbate, J.C. Fuggle, A. Fujimori, L.H. Tjeng, C.T. Chen, R. Potze, G.A. Sawatzky, H. Eisaki, S. Uchida, Phys. Rev. B 47 (1993) 16124.
[18] P. Ravindran, H. Fjellvag, A. Kjekshus, P. Blaha, K. Schwarz, J. Luitz, Web article, arXiv:cond-mat/0104308v1, April 17, 2001.
[19] I.A. Nekrasov, S.V. Streltsov, M.A. Korotin, V.I. Anisimov, Phys. Rev. B 68 (2003) 235113–235121.
[20] G.W.H. Hohne, W.F. Hemminger, H.-J. Flammershein, Differential Scanning Calorimetry, 2nd ed., Springer, Berlin, 2003.
[21] I. Barin, Thermochemical Data of Pure Substances, vols. I and II, 3rd ed., VCH, New York, 1995.
[22] G. Grønvold, E.J. Samuelsen, J. Phys. Chem. Solids 36 (1975) 249.
[23] B.H. Justice, E.F. Westrum Jr., J. Phys. Chem. 67 (1963) 339.
[24] B.H. Justice, E.F. Westrum Jr., J. Phys. Chem. 67 (1963) 345.
[25] E.F. Westrum Jr., B.H. Justice, J. Phys. Chem. 67 (1963) 659.